Nonequilibrium Criticality in Quench Dynamics of Long-Range Spin Models

Paraj Titum[1,2,3] and Mohammad F. Maghrebi[4]
[1]Johns Hopkins University Applied Physics Laboratory, Laurel, Maryland 20723, USA
[2]Joint Quantum Institute, NIST/University of Maryland, College Park, Maryland 20742, USA
[3]Joint Center for Quantum Information and Computer Science, NIST/University of Maryland, College Park, Maryland 20742, USA
[4]Department of Physics and Astronomy, Michigan State University, East Lansing, Michigan 48824, USA

(Received 5 November 2019; revised 7 June 2020; accepted 19 June 2020; published 21 July 2020)

Long-range interacting spin systems are ubiquitous in physics and exhibit a variety of ground-state disorder-to-order phase transitions. We consider a prototype of infinite-range interacting models known as the Lipkin-Meshkov-Glick model describing the collective interaction of N spins and investigate the dynamical properties of fluctuations and correlations after a sudden quench of the Hamiltonian. Specifically, we focus on critical quenches, where the initial state and/or the postquench Hamiltonian are critical. Depending on the type of quench, we identify three distinct behaviors where both the short-time dynamics and the stationary state at long times are effectively thermal, quantum, and genuinely nonequilibrium, characterized by distinct universality classes and static and dynamical critical exponents. These behaviors can be identified by an infrared effective temperature that is finite, zero, and infinite (the latter scaling with the system size as $N^{1/3}$), respectively. The quench dynamics is studied through a combination of exact numerics and analytical calculations utilizing the nonequilibrium Keldysh field theory. Our results are amenable to realization in experiments with trapped-ion experiments where long-range interactions naturally arise.

DOI: 10.1103/PhysRevLett.125.040602

The dynamics of isolated quantum systems has intrigued physicists since the dawn of quantum mechanics [1]. Furthermore, this topic has been in the spotlight in the past 2 decades thanks to the experimental advances in ultracold atoms [2–4] and trapped ions [5] among others [6,7]. These platforms are some of the prominent candidates for quantum simulation and well suited to investigate the dynamics away from equilibrium. A typical experimental setting is one where a system parameter suddenly changes—a scenario described as a quantum quench.

There is mounting evidence, both theoretical and experimental, that generic nonintegrable systems thermalize upon a quantum quench and local correlations are best described by a finite-temperature ensemble [8–10]. On the other hand, integrable systems defined by an extensive set of conserved quantities fail to thermalize and are often described by generalized Gibbs ensembles [11–15]. But even integrable systems often thermalize in a weaker sense of thermalization if their *long-wavelength* properties are described by a finite effective temperature. For example, such effective thermal behavior has been identified in one-dimensional condensates [16–21] and even observed in experiments [22,23]; similar behavior is predicted in integrable $O(N \to \infty)$ models [24–28]. This weaker notion of thermalization (with obvious merits for critical properties) is one that we adopt in this Letter. A natural question is then if, upon a quantum quench and depending on the initial state, even integrable systems always thermalize at long wavelengths, or, alternatively, can they exhibit genuinely nonequilibrium (critical) behavior?

In this Letter, we consider the quench dynamics of the Lipkin-Meshkov-Glick (LMG) model, an integrable model of spins with long-range interactions. This model has been used to model a variety of systems with applications to nuclear physics [29], Bose-Einstein condensates [30], small ferromagnetic particles [31], trapped ions [32–34], and ultracold atoms [35]. Recent research has focused on the dynamical aspects of this model [36–40]. We focus on the role of critical fluctuations and their universal properties. Our work sheds light on the nature of thermalization near quantum critical points and the origin of universality in subsequent dynamics. We show that, depending on the nature of the initial state (disordered or critical), distinct universal behaviors emerge in the dynamics. In particular, we show that fluctuations within the stationary state at late times can be described by an effective temperature which drastically depends on the initial state, and may vanish or even diverge for a quench from a critical state. The latter divergence is a signature of genuine nonequilibrium critical behavior.

We first emphasize what distinguishes our results from previous work. Conventionally, quench dynamics in the LMG model has been investigated with the spins initially in the ordered phase where the dynamics is governed by

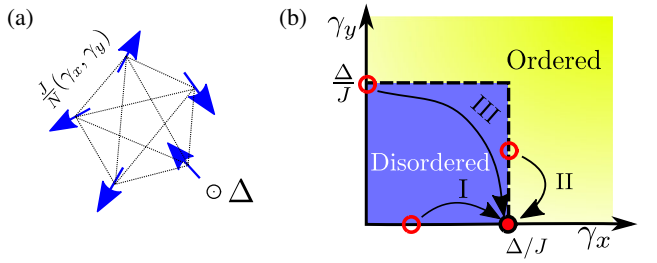

FIG. 1. (a) Schematic of the LMG model [Eq. (1)]. Spins interact via anisotropic XY Hamiltonian parametrized by $J(\gamma_x, \gamma_y)$ with a transverse magnetic field Δ. (b) Ground-state phase diagram of the LMG model. The critical (dashed) line defines the disorder-to-order transition. Three different initial states, corresponding to type-I, type-II, and type-III quenches, are shown as open circles, and the postquench Hamiltonian is denoted by a solid circle.

mean-field equations [34,41–45]. In contrast, we consider quenches where the order parameter is zero and dynamics lies solely in fluctuations beyond mean field. Quench dynamics near critical points have also been explored extensively in the context of the Kibble-Zurek mechanism [46,47] as the system is ramped through a quantum critical point [36,40,48–50]. This mechanism is commonly used to describe dynamics of slow quenches, or fast but shallow quenches, setting it apart from our work.

Model.—We consider a prototypical model of long-range interactions known as the LMG model [see Fig. 1(a)] whose Hamiltonian is given by

$$H = -\frac{J}{N}\sum_{i<j}\gamma_x\sigma_i^x\sigma_j^x + \gamma_y\sigma_i^y\sigma_j^y - \Delta\sum_i \sigma_i^z, \qquad (1)$$

with the interaction characterized by $\gamma_{x,y}$ and the transverse field Δ. The collective nature of the model allows us to write the Hamiltonian in terms of the total spin operators $S_a = \frac{1}{2}\sum_i \sigma_i^a$, with $a = x, y, z$. Note that the Hamiltonian commutes with $\mathbf{S}^2 = S_x^2 + S_y^2 + S_z^2$, making it block diagonal in a basis defined by the total spin S. In fact, this model is integrable [51] and exactly solvable using Bethe ansatz [52,53].

The ground-state phase diagram of the LMG model [Fig. 1(b)] exhibits a transition from a disordered paramagnet to an ordered ferromagnet [54–57]. The in-plane magnetization serves as an order parameter where $\langle S_x\rangle/N \neq 0$ and/or $\langle S_y\rangle/N \neq 0$ in the ordered phase while $\langle S_{x,y}\rangle/N = 0$ in the disordered phase, in the thermodynamic limit $N \to \infty$. The two phases are separated by a continuous transition along $\Delta = J\max\{\gamma_x, \gamma_y\}$. Given the infinite-range interactions, the phase diagram can be obtained from a mean-field analysis. However, mean-field theory is insufficient where the order parameter is zero (outside the ordered phase) and particularly fails to capture the divergent fluctuations at the critical point. These fluctuations scale with N as [58,59]

$$\frac{1}{N}\langle S_x^2\rangle \sim N^{1/3}, \qquad \frac{1}{N}\langle S_y^2\rangle \sim N^{-1/3}, \qquad (2)$$

along the critical line $\gamma_x > \gamma_y$; here, the prefactor $1/N$ factors out the trivial (square-root-volume) scaling away from criticality. Notice that the normalized spin fluctuations diverge only along the direction with the larger interaction strength. The exponent $1/3$ is a distinct signature of the quantum phase transition [58,59]. In contrast at a finite-temperature phase transition, the latter fluctuations diverge with a different critical exponent of $1/2$ [60]. Therefore, critical exponents distinguish between the quantum and thermal phase transitions of the LMG model.

Quench dynamics.—The LMG model being integrable does not fully thermalize; nonetheless, a generic quench gives rise to an effectively thermal behavior including critical exponents, as we shall see later. The question, however, remains if effective thermalization can be evaded at all, and, specifically, if a new, nonthermal critical behavior could emerge. Remarkably, the answer is in the affirmative. To show this, we study the dynamics for different types of quenches and initial states. To expose the critical behavior, the postquench Hamiltonian is considered to be one at a critical point; without loss of generality, we take $\{\gamma_x = 1, \gamma_y = 0, \Delta = J\}$. We consider three different initial states, each corresponding to the ground state of the LMG Hamiltonian but at different parameters: (i) type I, initial state deep in the disordered phase; (ii) type II, critical initial state on the critical line $\Delta = \gamma_x J$; (iii) type III, critical initial state on the critical line $\Delta = \gamma_y J$; see Fig. 1(b). Types II and III are distinguished by their initial divergent fluctuations in S_x and S_y, respectively.

It is instructive to first discuss a quench within the disordered phase, where we can make the Holstein-Primakoff approximation [61]. Rewriting the spin variables in terms of position and momentum, $S_x \approx \sqrt{N/2}x$ and $S_y \approx -\sqrt{N/2}p$, the LMG Hamiltonian (1) is recast as a harmonic oscillator with frequency $\Omega^2 \equiv 4\Delta^2(1 - J\gamma_x/\Delta)(1 - J\gamma_y/\Delta)$ and mass $2m \equiv 1/(\Delta - \gamma_y J)$ [62]. In this picture, the quench corresponds to a sudden change of the mass and frequency of the oscillator, $\{m_0, \Omega_0\} \to \{m, \Omega\}$. The long-time fluctuations following a quench to the vicinity of the critical point ($m\Omega \ll m_0\Omega_0$) are [62]

$$\frac{1}{N}\langle S_x^2(t)\rangle_{t\to\infty} = \frac{1}{2}\langle x^2(t)\rangle_{t\to\infty} \approx \frac{m_0\Omega_0}{8m^2\Omega^2}. \qquad (3)$$

This expression is reminiscent of a high-temperature harmonic oscillator ($T \gg \Omega$) where the equipartition theorem dictates $\frac{1}{2}m\Omega^2\langle x^2\rangle \approx \frac{1}{2}T$. This hints at the emergence of an effective temperature $T_{\text{eff}} = m_0\Omega_0/4m$ [25], or, equivalently,

$$T_{\mathrm{eff}} = \frac{\Delta}{2}\sqrt{\frac{\Delta_0 - J\gamma_{x0}}{\Delta_0 - J\gamma_{y0}}}. \tag{4}$$

Further insight is obtained by examining the behavior of T_{eff} for the different quenches. For the type-I quench, the initial state is disordered ($\Delta_0 > J\gamma_{x0}, J\gamma_{y0}$), giving rise to a finite effective temperature. For a type-II quench, the initial state is critical ($\Delta_0 = J\gamma_{x0} > J\gamma_{y0}$), resulting in a vanishing effective temperature. Surprisingly, for the type-III quench, the critical initial state ($\Delta_0 = J\gamma_{y0} > J\gamma_{x0}$) leads to a divergent effective temperature. This simple analysis hints at qualitatively different behaviors in types I, II, and III, which we will identify with an effective thermal, quantum, and nonequilibrium critical behavior, respectively. To this end, we go beyond the Holstein-Primakoff approximation both numerically using exact diagonalization and analytically via the Keldysh field theory.

First, we introduce universal scaling functions that capture the dynamics of the correlations and fluctuations,

$$\frac{1}{N}\langle S_x^2(t)\rangle = N^{\alpha} f\left(\frac{t}{N^{\zeta}}\right), \tag{5a}$$

$$C = \frac{1}{2N}\langle [S_x(t_2), S_x(t_1)]_+\rangle_{\mathrm{st}} = N^{\alpha}\tilde{C}\left(\frac{t_2 - t_1}{N^{\zeta}}\right), \tag{5b}$$

$$\chi = \frac{1}{2iN}\langle [S_x(t_2), S_x(t_1)]_-\rangle_{\mathrm{st}} = N^{\zeta}\tilde{\chi}\left(\frac{t_2 - t_1}{N^{\zeta}}\right), \tag{5c}$$

where f, $\tilde{C}$, $\tilde{\chi}$ are scaling functions. The two-time correlators C and χ denote the correlation and response functions, respectively, which in equilibrium are related via the fluctuation-dissipation relation (FDR) [63]. The subscript (st) indicates the long-time limit ($t_1, t_2 \gg |t_1 - t_2|$) when a stationary state is approached. We introduce two critical exponents: ζ describing the scaling of dynamics with system size and α characterizing the scaling of fluctuations. Remarkably, we see that these exponents describe the entire dynamics both at short times and the long-time stationary state. In the Supplemental Material, we also describe the scaling behavior of the two-time correlators in frequency space [62].

Numerical results.—Let us discuss the numerical results for the quench dynamics in the LMG model. The total-spin conservation allows us to simulate dynamics using exact diagonalization for large system sizes up to $N = 9000$ by restricting ourselves to the largest spin sector $S = N/2$ which also contains the ground state. Setting $J = 1$, we consider the postquench Hamiltonian with parameters $\{\gamma_x = 1, \gamma_y = 0, \Delta = 1\}$, and the initial states as the ground state of the Hamiltonian with the following parameters: (i) type I, $\{\gamma_x = 1, \gamma_y = 0, \Delta = 4\}$; (ii) type II, $\{\gamma_x = 1, \gamma_y = 0.5, \Delta = 1\}$; (iii) type III, $\{\gamma_x = 0, \gamma_y = 1, \Delta = 1\}$.

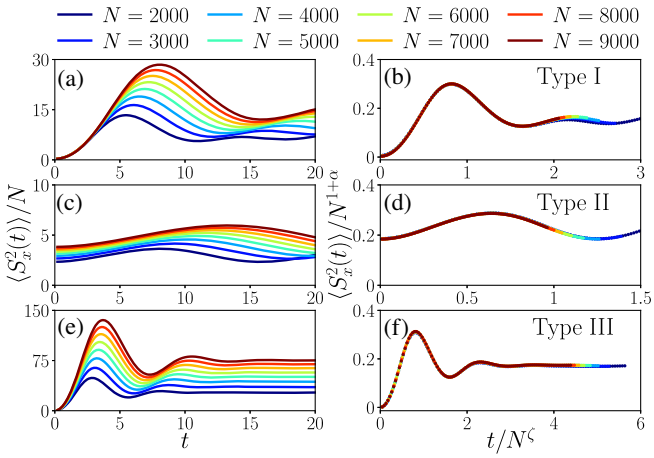

FIG. 2. Evolution of fluctuations, $(1/N)\langle S_x^2\rangle$, for quench types I, II and III (see Fig. 1) reported in the first [(a)–(b)], second [(c)–(d)] and third [(e)–(f)] rows, respectively. The right column shows the rescaled fluctuations and dynamics with the critical exponents (α, ζ) [see Eq. (5)] given by $(1/2, 1/4)$ [panel (b)] $(1/3, 1/3)$ [panel (d)] and $(2/3, 1/6)$ [panel (f)] corresponding to types I, II and III, respectively.

The evolution of fluctuations is plotted in Fig. 2, where each row corresponds to a given quench type. For a type-I quench [Figs. 2(a) and 2(b)], the initial state is in the disordered phase with small (i.e., noncritical) fluctuations. Fluctuations grow initially ($t \lesssim 1/J$) independent of the system size, but peak later at times that increase with the system size. The scaling collapse of the different curves [Fig. 2(b)] indicates that fluctuations diverge as $N^{0.5}$ and furthermore evolve with a characteristic time scale $\sim N^{0.25}$ before reaching the stationary state; hence, we identify the exponents $\zeta = 0.25$ and $\alpha = 0.5$. Indeed, the same exponents govern the two-time correlators in the stationary state consistent with the scaling in Eq. (5); see Supplemental Material [62]. Interestingly, these exponents are *identical* to those governing a thermal critical point [60]. This might be surprising because a true thermal phase transition only occurs at $\Delta/J < 1$ [66] in contrast with $\Delta/J = 1$ chosen above; hence the stationary state cannot be described as a Gibbs state [15]. This is also a consequence of integrability of the model. However, the fact that the critical behavior is consistent with a thermal phase transition hints at an *effective* thermalization at low frequencies.

For the type-II quench, the initial state is critical with divergent fluctuations in S_x. As shown in Fig. 2(c), fluctuations do not significantly grow over time. This observation indicates that the sudden quench has only slightly disturbed the system. Indeed, the scaling collapse shown in Fig. 2(d) reveals the exponents $\zeta = 0.33$ and $\alpha = 0.33$, consistent with a quantum critical behavior already present in the initial state. The emergence of quantum criticality in a quench from a critical state is also observed in the $O(N)$ model at large N [67].

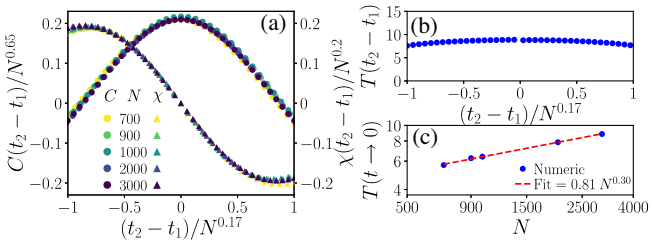

FIG. 3. (a) The correlation and response functions within the stationary state for the type-III quench for different system sizes. $t_2 = 20$ is chosen to ensure that the stationary state is reached. Scaling collapse is consistent with the exponents $\zeta = 1/6$ and $\alpha = 2/3$. (b) Time-dependent effective temperature $T(t)$ extracted from the two-time correlators for $N = 3000$ shown in (a). (c) Scaling of $T(t)$ with system size in the limit $t \to 0$. It is consistent with $T(t \to 0) \sim N^{1/3}$.

Most interestingly, the type-III quench exhibits novel nonequilibrium behavior that is neither thermal nor quantum critical. As shown in Fig. 2(e), fluctuations grow faster than the other quenches. While the dynamics might seem similar to the type-I quench, the exponents are markedly different: $(\zeta, \alpha) = (0.17, 0.67)$. This indicates that fluctuations diverge with the system size even more strongly than those in type I or, equivalently, at the thermal critical point. Indeed, as we shall see shortly, the effective temperature in this case diverges with the system size. We also compute the two-time correlators for this quench as shown in Fig. 3(a). Again, we find that the correlation and response functions obey the scaling forms in Eqs. (5b) and (5c) with approximately the same critical exponents.

In equilibrium, the FDR dictates $C(\omega) = (2T/\omega)i\chi(\omega)$ at finite temperature and low frequencies [63]. We use this relation to define an effective temperature outside equilibrium: $T_{\rm eff}(\omega) \equiv \omega C(\omega)/2i\chi(\omega)$, with the low-frequency limit $T_{\rm eff}^{\rm IR} = \lim_{\omega\to 0} T_{\rm eff}(\omega)$. However, it is difficult to access numerically, so we take an alternative approach by using the FDR in the time domain, $\chi(t) = (1/2T)\partial_t C(t)$ with t the time difference. We identify a time-dependent effective temperature, $T(t) \equiv \partial_t C(t)/2\chi(t)$ [68]. Note that $T(t)$ is *not* the Fourier transform of the effective temperature $T_{\rm eff}(\omega)$; however, it is expected to exhibit similar scaling behavior [62]. Now for the type-III quench, the two-time correlators in Fig. 3(a) give rise to the time-dependent effective temperature $T(t)$ in Fig. 3(b). In Fig. 3(c), we show that this temperature scales with system size, $T(t \to 0) \sim N^{1/3}$, consistent with the scaling relations in Eqs. (5b) and (5c) for type III [62]. This scaling should be contrasted with the constant effective temperature for the type-I quench [62].

Scaling analysis.—Scaling relations postulated in Eqs. (5a)–(5c) and observed in numerics can be obtained from an effective low-frequency theory. At (or near) the critical point of the postquench Hamiltonian, the relevant degree of freedom is x, which also serves as the order parameter within the ordered phase; see discussion above Eq. (3). The dynamics is governed by the Hamiltonian $H = p^2/2m + \frac{1}{2}m\Omega^2 x^2 + (u/2N)x^4$, with $u \equiv J\gamma_x$, where we have included the relevant nonlinear interactions beyond the harmonic terms [62]. To describe the nonequilibrium dynamics, we shall utilize the Schwinger-Keldysh path integral over forward $[x_+(t)]$ and backward $[x_-(t)]$ trajectories weighted by $e^{i(S[x_+]-S[x_-])}$ with S the corresponding action $S[x(t)] = \int dt[\frac{1}{2}m\dot{x}^2 - \frac{1}{2}m\Omega^2 x^2 - (u/2N)x^4]$:

$$Z = \int [dx_\pm] W_0 e^{i(S[x_+]-S[x_-])}. \tag{6}$$

Here, W_0 is the Wigner function describing the initial state. Introducing the variables $x_{c/q} = (x_+ \pm x_-)/\sqrt{2}$, the "Keldysh action" becomes $S_K \equiv S[x_+] - S[x_-] = -\int_0^\infty dt[m x_q \ddot{x}_c + r x_q x_c + (u/N)(x_c^2 + x_q^2)x_c x_q]$, with $r \equiv m\Omega^2$. The N dependence of the Wigner function is given by $W_0 = \mathcal{W}(x_{c0}^2 N^{-\alpha_0}, \dot{x}_{c0}^2 N^{\alpha_0})$, where $\mathcal{W}(\cdot,\cdot)$ is an N-independent function that is significant when its arguments are $\lesssim 1$ [62]; the form of $\mathcal{W}$ can be traced to that of the ground-state wave function of a particle in a quadratic (type I) or quartic (types II and III) potential [69]. The subscript 0 denotes initial values and $\alpha_0 = 0, 1/3, -1/3$ distinguish types I, II, and III, respectively [62]. This reproduces fluctuations in the initial state $\langle x^2 \rangle \sim N^{\alpha_0}$ (similarly for p); see Eq. (2). Note that, due to integrability, no dissipation ($\sim \int_t x_q \dot{x}_c$) arises in the Keldysh action.

We focus on obtaining critical exponents for types I and III where $\alpha_0 \le 0$ and the system is significantly disturbed upon quench. We do so by identifying a scale-invariant fixed point (i.e., independent of N) of the Keldysh action along with the initial state. For quenches to the critical point, $r = 0$, we expect (confirmed by numerics) a divergence in fluctuations, $\langle S_x^2 \rangle/N \sim \langle x_c^2 \rangle \sim N^\alpha$ and a critical slowdown, $t \sim N^\zeta$, with exponents α, $\zeta > 0$ to be determined. Defining scaled variables $X_c = x_c N^{-\alpha/2}$ and $T = tN^{-\zeta}$ and appropriately choosing these exponents, the action together with the Wigner function can be made scale invariant. In terms of the scaled variables, $W_0 = \mathcal{W}(X_{c0}^2 N^{\alpha-\alpha_0}, X_{c0}'^2 N^{\alpha-2\zeta+\alpha_0})$ with $X' = dX/dT$. For the quenches under consideration, $\alpha - \alpha_0 > 0$ and $\mathcal{W}$, only significant for arguments of order 1, is negligible due a divergent argument unless $X_{c0} \approx 0$. Moreover, fluctuations of X_{c0}' and thus the Wigner function can be made scale invariant by setting $\alpha - 2\zeta + \alpha_0 = 0$. Similar analysis can be done at the level of the action. The kinetic term ($\sim \int_t x_q \ddot{x}_c$) is made scale invariant by introducing a rescaled variable $X_q = N^{-\alpha/2+\zeta} x_q$. The interaction, $(-1/N)\int_t u_c x_q x_c^3 + u_q x_q^3 x_c$, comprises "classical" ($\sim u_c$) and "quantum" ($\sim u_q$) vertices although $u_c = u_q$ at the microscopic level. Recasting the classical vertex in terms of the rescaled variables, we have $u_c/N \to u_c N^{2\zeta+\alpha-1}$, which becomes scale invariant when $2\zeta + \alpha - 1 = 0$. Under these scaling transformations, the quantum vertex is suppressed by

TABLE I. Critical exponents ζ and α characterizing the scaling of dynamics and fluctuations, respectively. Distinct critical behaviors emerge in quench types I, II, and III. Types I and II give identical exponents as thermal and quantum critical points (TCP and QCP), respectively. Genuinely nonequilibrium exponents emerge in type III. The IR limit ($\omega \to 0$) of the effective temperature is finite, zero, and divergent for these three quenches, respectively.

	Type I	Type II	Type III	TCP	QCP
ζ	$\frac{1}{4}$	$\frac{1}{3}$	$\frac{1}{6}$	$\frac{1}{4}$	$\frac{1}{3}$
α	$\frac{1}{2}$	$\frac{1}{3}$	$\frac{2}{3}$	$\frac{1}{2}$	$\frac{1}{3}$
$T_{\mathrm{eff}}^{\mathrm{IR}}$	Finite	0	$\sim N^{1/3}$	T_c	0

N and becomes irrelevant. In contrast to types I and III, the type-II quench ($\alpha_0 > 0$) acts as a marginal perturbation of a critical system; hence the quantum critical behavior persists [62]. Finally, combining the above relations, the critical exponents are determined as $\zeta = (1 + \alpha_0)/4$ and $\alpha = (1 - \alpha_0)/2$. Our scaling analysis yields the exponents listed in Table I consistent with numerics, and also reproduces the scaling of the effective temperature [62]. We remark that, in analogy with boundary critical phenomena [70,71], our analysis has relied on scaling both "boundary" and "bulk" terms. Here, we have focused on finite-size scaling, but we can also identify the scaling behavior in the thermodynamic limit ($N \to \infty$) away from the critical point [62].

The nonequilibrium dynamics reported in this Letter is accessible in a variety of experimental platforms, particularly in the context of trapped ions [5,32,34], which are described by spin models with long- or even infinite-range interactions. A challenge is to prepare an initial critical state for type-II and type-III quench dynamics. However, based on a quantum approximate optimization protocol [72], variational quantum algorithms have been recently proposed [73] and implemented [74] to efficiently prepare quantum critical states.

Conclusion and outlook.—In this Letter, we have identified scenarios where genuinely nonequilibrium critical behavior emerges in the dynamics of integrable quantum systems. The infinite-range nature of the LMG model is particularly useful in our analytical and numerical analysis; however, short-range integrable systems such as the $O(N \to \infty)$ model [25,67] and free fermions also exhibit analogs of types I and II. Additionally, similar behavior should be expected for long-range spin models, $V(r) \sim 1/r^p$ specifically with $p < 1$, which, though not integrable, give rise to long-lived prethermal states [75]. Extending our results to other integrable models or those exhibiting long-lived prethermalization is worthwhile. Finally, it would be interesting to identify *aging* behavior [76] in such models.

We thank Marcos Rigol and Daniel Paz for useful discussions. P. T. acknowledges support from the NIST NRC Research Postdoctoral Associateship Award. M. F. M. acknowledges support from NSF under Grant No. DMR-1912799 and start-up funding from Michigan State University. This work is supported in part by the U.S. Department of Energy (DOE), Office of Science, Office of Advanced Scientific Computing Research (ASCR) Quantum Computing Application Teams program, under fieldwork Proposal No. ERKJ347. The authors acknowledge the University of Maryland supercomputing resources [77] made available for conducting the research reported in this Letter. This research was supported in part by the National Science Foundation under Grant No. NSF PHY-1748958.

[1] J. von Neumann, Z. Phys. **57**, 30 (1929).
[2] I. Bloch, J. Dalibard, and W. Zwerger, Rev. Mod. Phys. **80**, 885 (2008).
[3] A. Polkovnikov, K. Sengupta, A. Silva, and M. Vengalattore, Rev. Mod. Phys. **83**, 863 (2011).
[4] T. Langen, R. Geiger, and J. Schmiedmayer, Annu. Rev. Condens. Matter Phys. **6**, 201 (2015).
[5] R. Blatt and C. F. Roos, Nat. Phys. **8**, 277 (2012).
[6] P. Schauss, Quantum Sci. Technol. **3**, 023001 (2018).
[7] D. E. Chang, J. S. Douglas, A. González-Tudela, C.-L. Hung, and H. J. Kimble, Rev. Mod. Phys. **90**, 031002 (2018).
[8] L. D'Alessio, Y. Kafri, A. Polkovnikov, and M. Rigol, Adv. Phys. **65**, 239 (2016).
[9] C. Gogolin and J. Eisert, Rep. Prog. Phys. **79**, 056001 (2016).
[10] M. Srednicki, J. Phys. A **32**, 1163 (1999).
[11] A. C. Cassidy, C. W. Clark, and M. Rigol, Phys. Rev. Lett. **106**, 140405 (2011).
[12] J.-S. Caux and R. M. Konik, Phys. Rev. Lett. **109**, 175301 (2012).
[13] M. Fagotti and F. H. L. Essler, Phys. Rev. B **87**, 245107 (2013).
[14] J. Sirker, N. P. Konstantinidis, F. Andraschko, and N. Sedlmayr, Phys. Rev. A **89**, 042104 (2014).
[15] L. Vidmar and M. Rigol, J. Stat. Mech. (2016) 064007.
[16] A. Lamacraft, Phys. Rev. Lett. **98**, 160404 (2007).
[17] R. Bistritzer and E. Altman, Proc. Natl. Acad. Sci. U.S.A. **104**, 9955 (2007).
[18] T. Kitagawa, A. Imambekov, J. Schmiedmayer, and E. Demler, New J. Phys. **13**, 073018 (2011).
[19] K. Agarwal, E. G. Dalla Torre, B. Rauer, T. Langen, J. Schmiedmayer, and E. Demler, Phys. Rev. Lett. **113**, 190401 (2014).
[20] K. Agarwal, E. G. Dalla Torre, J. Schmiedmayer, and E. Demler, Phys. Rev. B **95**, 195157 (2017).
[21] E. Altman,arXiv:1512.00870.
[22] M. Gring, M. Kuhnert, T. Langen, T. Kitagawa, B. Rauer, M. Schreitl, I. Mazets, D. A. Smith, E. Demler, and J. Schmiedmayer, Science **337**, 1318 (2012).
[23] D. A. Smith, M. Gring, T. Langen, M. Kuhnert, B. Rauer, R. Geiger, T. Kitagawa, I. Mazets, E. Demler, and J. Schmiedmayer, New J. Phys. **15**, 075011 (2013).
[24] A. Chandran, A. Nanduri, S. S. Gubser, and S. L. Sondhi, Phys. Rev. B **88**, 024306 (2013).

[25] A. Chiocchetta, M. Tavora, A. Gambassi, and A. Mitra, Phys. Rev. B **91**, 220302(R) (2015).
[26] P. Smacchia, M. Knap, E. Demler, and A. Silva, Phys. Rev. B **91**, 205136 (2015).
[27] A. Chiocchetta, M. Tavora, A. Gambassi, and A. Mitra, Phys. Rev. B **94**, 134311 (2016).
[28] A. Mitra, Annu. Rev. Condens. Matter Phys. **9**, 245 (2018).
[29] H. Lipkin, N. Meshkov, and A. Glick, Nucl. Phys. **A62**, 188 (1965).
[30] J. I. Cirac, M. Lewenstein, K. Mølmer, and P. Zoller, Phys. Rev. A **57**, 1208 (1998).
[31] E. M. Chudnovsky and L. Gunther, Phys. Rev. Lett. **60**, 661 (1988).
[32] J. W. Britton, B. C. Sawyer, A. C. Keith, C.-C. J. Wang, J. K. Freericks, H. Uys, M. J. Biercuk, and J. J. Bollinger, Nature (London) **484**, 489 (2012).
[33] J. G. Bohnet, B. C. Sawyer, J. W. Britton, M. L. Wall, A. M. Rey, M. Foss-Feig, and J. J. Bollinger, Science **352**, 1297 (2016).
[34] J. Zhang, G. Pagano, P. W. Hess, A. Kyprianidis, P. Becker, H. Kaplan, A. V. Gorshkov, Z.-X. Gong, and C. Monroe, Nature (London) **551**, 601 (2017).
[35] V. Makhalov, T. Satoor, A. Evrard, T. Chalopin, R. Lopes, and S. Nascimbene, Phys. Rev. Lett. **123**, 120601 (2019).
[36] M.-J. Hwang, R. Puebla, and M. B. Plenio, Phys. Rev. Lett. **115**, 180404 (2015).
[37] A. Lerose, J. Marino, B. Žunkovič, A. Gambassi, and A. Silva, Phys. Rev. Lett. **120**, 130603 (2018).
[38] A. Relaño, Phys. Rev. Lett. **121**, 030602 (2018).
[39] J. Lang, B. Frank, and J. C. Halimeh, Phys. Rev. Lett. **121**, 130603 (2018).
[40] N. Defenu, T. Enss, M. Kastner, and G. Morigi, Phys. Rev. Lett. **121**, 240403 (2018).
[41] S. Campbell, Phys. Rev. B **94**, 184403 (2016).
[42] B. Žunkovič, A. Silva, and M. Fabrizio, Phil. Trans. R. Soc. A **374**, 20150160 (2016).
[43] T. Mori, Phys. Rev. E **96**, 012134 (2017).
[44] I. Homrighausen, N. O. Abeling, V. Zauner-Stauber, and J. C. Halimeh, Phys. Rev. B **96**, 104436 (2017).
[45] B. Žunkovič, M. Heyl, M. Knap, and A. Silva, Phys. Rev. Lett. **120**, 130601 (2018).
[46] W. H. Zurek, Nature (London) **317**, 505 (1985).
[47] T. W. B. Kibble, J. Phys. A **9**, 1387 (1976).
[48] A. Polkovnikov, Phys. Rev. B **72**, 161201(R) (2005).
[49] A. Polkovnikov and V. Gritsev, Nat. Phys. **4**, 477 (2008).
[50] T. Caneva, R. Fazio, and G. E. Santoro, Phys. Rev. B **78**, 104426 (2008).
[51] P. Leboeuf and A. Voros, J. Phys. A **23**, 1765 (1990).
[52] F. Pan and J. Draayer, Phys. Lett. B **451**, 1 (1999).
[53] H. Morita, H. Ohnishi, J. da Providência, and S. Nishiyama, Nucl. Phys. **B737**, 337 (2006).
[54] R. Botet and R. Jullien, Phys. Rev. B **28**, 3955 (1983).
[55] S. Dusuel and J. Vidal, Phys. Rev. Lett. **93**, 237204 (2004).
[56] P. Ribeiro, J. Vidal, and R. Mosseri, Phys. Rev. Lett. **99**, 050402 (2007).
[57] P. Ribeiro, J. Vidal, and R. Mosseri, Phys. Rev. E **78**, 021106 (2008).
[58] F. Leyvraz and W. D. Heiss, Phys. Rev. Lett. **95**, 050402 (2005).
[59] J. Vidal and S. Dusuel, Europhys. Lett. **74**, 817 (2006).
[60] D. A. Paz and M. F. Maghrebi, arXiv:1906.08278.
[61] A. Das, K. Sengupta, D. Sen, and B. K. Chakrabarti, Phys. Rev. B **74**, 144423 (2006).
[62] See Supplemental Material at http://link.aps.org/supplemental/10.1103/PhysRevLett.125.040602 for additional details on the analytical results using Holstein-Primakoff approximation, Schwinger-Keldysh field theory and the scaling analysis, as well as numerical results for the two-time correlations in the type-I quench, which includes Refs. [63–65].
[63] U. C. Täuber, *Critical Dynamics* (Cambridge University Press, Cambridge, England, 2014).
[64] C. Gardiner and P. Zoller, *Quantum Noise* (Springer Science & Business Media, Heidelberg, Germany, 2004), Vol. 56.
[65] M. Foss-Feig, P. Niroula, J. T. Young, M. Hafezi, A. V. Gorshkov, R. M. Wilson, and M. F. Maghrebi, Phys. Rev. A **95**, 043826 (2017).
[66] B. K. Chakrabarti, S. Suzuki, and J.-i. Inoue, *Quantum Ising Phases and Transitions in Transverse Ising Models*, 2nd ed. (Springer-Verlag, Heidelberg, Germany, 2013).
[67] A. Chiocchetta, A. Gambassi, S. Diehl, and J. Marino, Phys. Rev. Lett. **118**, 135701 (2017).
[68] L. F. Cugliandolo, J. Phys. A **44**, 483001 (2011).
[69] P. Buonsante, R. Burioni, E. Vescovi, and A. Vezzani, Phys. Rev. A **85**, 043625 (2012).
[70] H. W. Diehl and S. Dietrich, Z. Phys. B **42**, 65 (1981).
[71] H. W. Diehl, Int. J. Mod. Phys. B **11**, 3503 (1997).
[72] E. Farhi, J. Goldstone, and S. Gutmann, arXiv:1411.4028.
[73] W. W. Ho and T. H. Hsieh, SciPost Phys. **6**, 29 (2019).
[74] D. Zhu, S. Johri, N. M. Linke, K. A. Landsman, N. H. Nguyen, C. H. Alderete, A. Y. Matsuura, T. H. Hsieh, and C. Monroe, arXiv:1906.02699.
[75] T. Mori, J. Phys. A **52**, 054001 (2019).
[76] P. Calabrese and A. Gambassi, J. Phys. A **38**, R133 (2005).
[77] See http://hpcc.umd.edu.